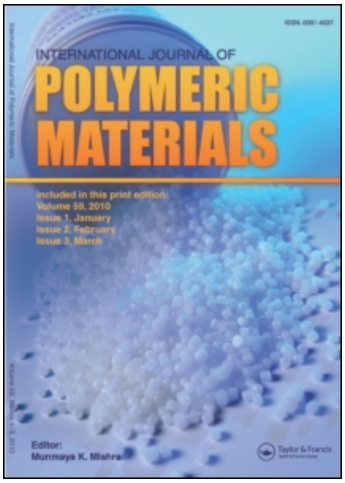

International Journal of Polymeric Materials
Publication details, including instructions for authors and subscription information:
http://www.informaworld.com/smpp/title~content=t713647664

Initiator Artifacts in the Emulsion and Microemulsion Copolymerization of Partially Water-Soluble Monomers

Sumit Bhawal[a]; Surekha Devi[a]; Deepa Dhoble[b]
[a] Department of Chemistry, Faculty of Science, M. S. University of Baroda, Baroda, India [b] Polymer Division, National Chemical Laboratory, Pune, India

To cite this Article Bhawal, Sumit , Devi, Surekha and Dhoble, Deepa(2005) 'Initiator Artifacts in the Emulsion and Microemulsion Copolymerization of Partially Water-Soluble Monomers', International Journal of Polymeric Materials, 55: 4, 255 — 281
To link to this Article: DOI: 10.1080/009140390945132
URL: http://dx.doi.org/10.1080/009140390945132

International Journal of Polymeric Materials, 55:255–281, 2006

ISSN: 0091-4037 print/1563-5333 online
DOI: 10.1080/009140390945132

Taylor & Francis
Taylor & Francis Group

Initiator Artifacts in the Emulsion and Microemulsion Copolymerization of Partially Water-Soluble Monomers

Sumit Bhawal
Surekha Devi
Department of Chemistry, Faculty of Science, M. S. University of Baroda, Baroda, India

Deepa Dhoble
Polymer Division, National Chemical Laboratory, Pune, India

The emulsion and microemulsion copolymerizations of partially water-soluble monomers ethylacrylate (EA) and methylmethacrylate (MMA) were studied with the water-soluble initiator KPS and the oil soluble initiator AIBN. On changing from an emulsion to microemulsion system the shift in relative contribution of the different phases involved in particle formation is expected to control the kinetic and colloidal parameters and hence the solid content and latex stability. This has been tested using the water-soluble initiator KPS and the oil-soluble initiator AIBN. The microemulsion system initiated with KPS resulted in a much higher particle size and lower particle stability, whereas the emulsion system initiated with KPS at identical reaction conditions resulted in a stable colloidal polymer particles of very low particle size at a higher solid content. On the contrary, AIBN-initiated microemulsion generated a stable nanolatex as compared to the emulsion system. The copolymers, isolated during the nucleation stage, were analyzed for their composition using ^1H NMR and for their thermal properties using DSC.

Keywords: polymerization, emulsion, microemulsion, ethylacrylate, methylmethacrylate

Received 15 January; in final form 24 January 2005.

The authors gratefully acknowledge the financial assistance by United Grants Commission, New Delhi, India. The authors are also grateful to Dr. S. Sivaram, Director, NCL, Pune for providing the Light Scattering facility.

Address correspondence to Surekha Devi, Department of Chemistry, Faculty of Science, M. S. University of Baroda, Baroda 390002, India. E-mail: surekha_devi@yahoo.com

INTRODUCTION

Polymerization in microemulsion medium is an attractive method for producing high molecular weight colloidal particles of ultra low particle size with a narrow particle size distribution [1]. The aforementioned features are due to a high degree of compartmentalization of the polymerization locus, which is achieved by employing a high surfactant concentration [2]. The polymerization locus for hydrophobic monomers like styrene has largely been reported to be the microemulsion droplet [3], whereas for partially water-soluble monomer like MMA evidence for homogeneous nucleation has also been reported [4–5]. Reduction in surfactant concentration transforms a transparent microemulsion to a turbid emulsion with a corresponding increase in the droplet size and decrease in the degree of compartmentalization. The larger droplets contribute very little to the overall particle nucleation [6].

However, a decrease in surfactant concentration shifts the relative contribution of the different phases involved in particle formation, particularly for polar monomers, affecting the number of particles, particle size, and its distribution and thus the latex stability. Many reports are available on the homopolymerization of polar monomers [7–8] but information regarding the copolymerization of partially water-soluble monomer pairs is still very scanty. Capek and Tuan [9] first reported emulsion copolymerisation of EA–MMA where they suggested initiation of polymerization in both aqueous and micellar phase. The present authors' earlier work on emulsion copolymerization of EA–MMA also provides experimental evidences in support of such a mechanism [10]. However, no reports are available on such copolymerization in microemulsion.

The present work discusses the microemulsion and emulsion copolymerization of EA–MMA, mainly to highlight the difference in the process of particle evolution in the two systems. Because both monomers partition between aqueous phase and droplets, choice of water soluble initiator KPS and oil soluble initiator AIBN might help in understanding the relative contribution of heterogeneous and homogeneous nucleation in emulsion and microemulsion systems.

EXPERIMENTAL

Materials

EA and MMA from National Chemicals, Baroda, India, were purified by passing through an alumina column followed by vacuum

distillation under reduced pressure and stored at 4°C till further use. Sodium dodecyl sulphate (SDS) extrapure from S.D. Fine Chemicals, Baroda, India was used as received. Potassium persulphate (KPS) from Sisco Chem., Mumbai, India, was recrystallized from distilled water before use. AIBN from S.D. Fine Chemicals, Baroda, India was recrystallized from a mixture of chloroform and methanol.

Polymerization Procedure

Kinetics

The batch polymerization in emulsion and microemulsion medium was carried out in a five-neck reaction kettle equipped with a mechanical stirrer, condenser, nitrogen gas inlet, and dropping funnel. The micellar solution containing water and surfactant was stirred for 30 min at the polymerization temperature. This was followed by the addition of monomer over 2 min. The mixture was further stirred for 15 min for emulsification. The requisite quantity of initiator KPS was added to the reaction mixture and the kinetics of the reaction was studied by withdrawing aliquots at regular time intervals. When AIBN was used as an initiator, it was predissolved in the monomer and added to the reaction mixture. The reaction was quenched by adding 40 ppm of hydroquinone. Percentage conversion was determined gravimetrically using methanol as a non-solvent. The kinetics of the reaction was studied at monomers/surfactant (M/S) ratio 0.66 (microemulsion) and at M/S ratio 10 and 50 (emulsion). The composition of the respective systems in weight percentages is

M/S = 0.66: 10 EA, 15 SDS, 80 water, and 0.18–0.73 mM KPS.
M/S = 10: 10 EA, 1 SDS, 89 water, and 0.18–0.73 mM KPS.
M/S = 50: 25 EA, 0.5 SDS, 74.5 water, and 0.18–0.73 mM KPS.
For AIBN the initiator concentration was varied from 0.30 mM–1.83 mM.

Characterisation

Particle Size Measurements

A Malvern Photon Correlation spectrophotometer, Model 4700, equipped with a vertically polarized argon ion laser source operating at 488 nm was used to measure the particle size of the polymerized latexes in dynamic mode. The scattering intensities from the sample were measured at 90° with the help of a photomultplier tube. Intensity correlation data were analysed by the method of cumulants to provide the average decay rate, $\langle \Gamma^2 \rangle = q^2 D$, where $q = (4\Pi n/\lambda) \sin\theta/2$ is

the scattering vector, n is the index of refraction, D the diffusion coefficient and the variance, $\nu = \langle\Gamma^2\rangle - \langle\Gamma\rangle^2/\langle\Gamma\rangle^2$, which is a measure of the width of the distribution of the decay rate. The measured diffusion coefficients were represented in terms of apparent radii by means of Stokes law. Latexes were diluted up to 100 times and filtered through 0.2 μm Millipore filters before measurements to minimize particle–particle interaction and remove dust particles. The number of particles were calculated using the following equation,

$$N_p = 6\,M_o\,X_m/\pi\,\rho\,D_n^3 \tag{1}$$

where D_n is a number average diameter of the polymer particles obtained from dynamic light scattering, X_m is fractional conversion; M_o is amount of monomer initially charged in g/cm^3; ρ is density of polymer in g/cm^3 and N_p is number of particles/cm^3.

Particle sizes of the polymer latexes at 97% conversion were also determined using a Philips Technai–20 transmission electron microscope operated at 200 Kv accelerating voltage. The polymerized latexes were diluted 100 times with deionized distilled water and one drop of the diluted dispersion was placed on 200-mesh carbon coated copper grid. Uranyl acetate 2% w/v was used as a staining agent. Diameters of at least 60 randomly chosen particles were measured directly from the micrograph. The number and weight average diameters were calculated using Equations 2 and 3 respectively, where D_i is the diameter of the particle and **n** is the number of particles measured.

$$D_n = \frac{\Sigma n_i\,D_i}{n} \tag{2}$$

$$D_w = \frac{\Sigma n_i\,D_i^4}{\Sigma n_i\,D_i^3} \tag{3}$$

Spectroscopic Analysis

The composition of the copolymer was determined from ^{1}H NMR spectra recorded on a 200 MHz Bruker DPX 200 instrument using TMS as an internal reference and 2% w/v sample solution in $CDCl_3$.

Thermal Analysis

Differential scanning calorimetric (DSC) analysis was carried out using a universal V.2.6D TA instrument at a heating rate of 10°C min^{-1}.

Molecular Weight Measurements

A Thermo–Quest GPC equipped with Spectra system RI 150 refractive index detector, As-300 auto sampler, and Spectra system P100 pump were used along with PSS–GPC software. HPLC grade THF from S.D. Fine Chemicals was used as a mobile phase at room temperature. The stationary phase consisted of two PL Gel SDV 5 μ linear and 100 Å (8×600 mm) columns. 20 μL of 0.1% polymer solutions were injected to get a neat chromatogram. Narrow molecular weight distribution PMMA samples (molecular weight range, 1.4×10^6 to 3.06×10^2) were used as calibrating standards.

RESULTS

Phase Diagram

The one phase region for oil/water (o/w) microemulsion was determined visually by titrating a mixture of EA and MMA (1:1 mole ratio) with different concentrations of SDS in water at 33°C and at the polymerization temperature 70°C. The compositions were thoroughly mixed using a vortex mixer. The dotted region in Figure 1 represents the clear but rather viscous region. Polymerizations of EA–MMA carried out at M/S ratios 0.66, 10, and 50 are represented by points A, B, C in the phase diagram.

Kinetic Study

The kinetics of the microemulsion polymerisations initiated with KPS were studied using 10% of the monomer and 15% surfactant. Beyond 12% monomer phase separation was observed. The microemulsion system initiated with KPS and AIBN showed the presence of gel effect around 70% conversion. The final particle size obtained from KPS-initiated systems was 160 nm, whereas that initiated with the same molar concentration of AIBN, temperature, and M/S ratio was observed to be 78 nm. Also, the particle size distribution for the microemulsion system initiated by KPS was broader than the AIBN-initiated system under identical reaction conditions. Copolymer composition studied at $<10\%$ conversion (nucleation stage) through ^{1}H NMR showed similar fractions of MMA and EA for both microemulsion and bulk at identical feed concentration. DSC results show a single Tg for samples below 10% conversion in microemulsion. The number and weight average molecular weight for the KPS-initiated system was lower in comparison to the AIBN-initiated system. The

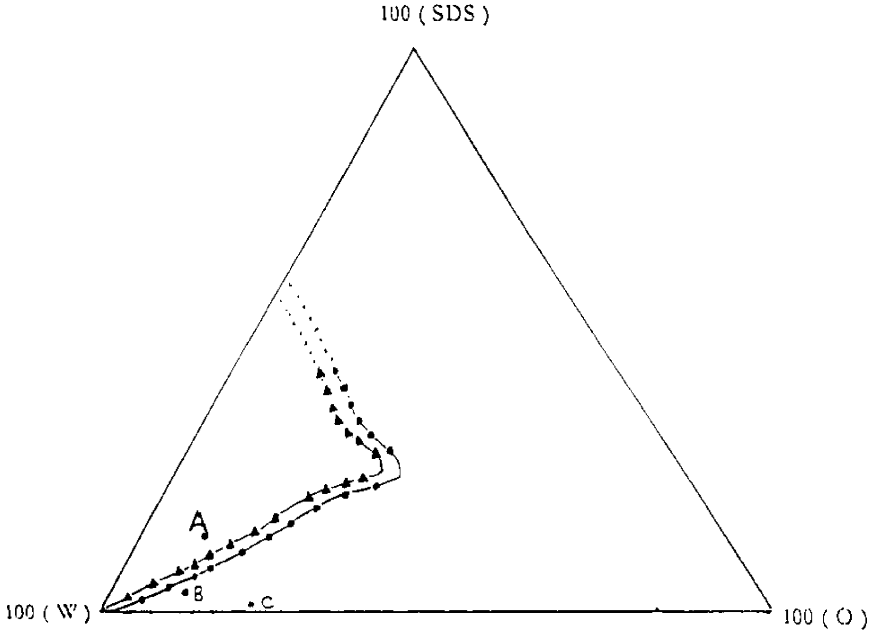

FIGURE 1 Phase diagram of EA (0.5)–MMA (0.5)/SDS/water system, (▲) at 34°C and (●) at 70°C.

molecular weight polydispersity was also higher for the KPS initiated system.

Surprisingly, KPS initiated emulsion polymerization of EA–MMA carried out with 10 and 25% of the monomer with 1 and 0.5% surfactant resulted in the production of stable translucent nanolatex with final particle size 42 and 61 nm, respectively. The particle size distribution was bimodal during the nucleation stage, whereas at higher conversion they were more monodispersed, especially for $M/S = 50$. Copolymer composition below 10% conversion showed by ^1H NMR a higher fraction of the more water soluble monomer EA in the copolymer, in comparison to bulk and microemulsion for identical feed. DSC results showed two Tgs for all compositions below 10% conversion in emulsion. The number of particles and rate of polymerization were found to be higher for emulsion system than in microemulsion at the same molar concentration of KPS. The AIBN-initiated system, on the contrary, resulted in phase separation at $M/S = 10$ and 50. However on increasing the initiator concentration to 12 mM, stable particles could be generated with a resulting particle size of 85 nm.

DISCUSSION

The transparent microemulsions represented by point A of the phase diagram ($M/S = 0.66$) became increasingly turbid as the reaction proceeded due to particle growth and increased difference in refractive index between polymer particles and suspending medium. Increase in initiator concentration yielded faster polymerization rates and higher conversion regardless of the type of initiator employed. The increase in polymerization rate with increase in initiator concentration is a consequence of higher free radical flux leading to higher probability of radical capture by droplets (heterogeneous nucleation) or by monomer dissolved in the aqueous phase, to produce particles in the aqueous phase (homogeneous nucleation). The dependency of the rate of polymerization on KPS in microemulsion and emulsion was observed to be 0.5 and 0.86, respectively. The relatively higher dependency for emulsion system (compared to microemulsion) can be explained on the basis of a greater sensitivity of polymerization rate on KPS concentration. The greater sensitivity is an artifact of higher rate of particle nucleation in the emulsion system than in the microemulsion. The Rp versus conversion plots (Figures 2 and 3) for both systems show the presence of gel effect, which is seen as a small hump around 60–70% conversion. The origin of the gel effect at higher weight fraction of the polymer might be due to the growth of shorter chains (largely responsible for termination) and decrease in their translational mobility due to increase in micro viscosity within the polymer particle. The increase in micro viscosity arises due to (i) solubility of polymer in the monomer (ii) Closeness of Tg of copolymer (66°C) and reaction temperature (70°C). The aforementioned factors can lead to the polymer radical to live longer before termination, especially if the active sites of the polymer chains are entrapped in a larger particle volume (also seen by the higher value of $\bar{n}$). If sufficient monomer is present in the vicinity, the earlier conditions will slow down the rate of termination (relative to propagation) because it is a diffusion-controlled process.

The time evolution of conversion for both KPS-and AIBN-initiated microemulsion is given in Figures 2 and 3. The maximum conversion achieved with KPS as initiator was around 80–85% after 3 h. The limiting conversion at 80–85% can be attributed to the decrease in pH to 3.6 at the end of polymerization from an initial pH of 7.2.

The decrease in pH may be due to the generation of bisulphate ions in addition to the free radicals produced from KPS decomposition. This results in decreased flux of the generated free radicals because the decomposition rate constant is reported to depend on the pH [11]. Hence, there is a possibility of initiator autoinhibition in persulphate-initiated

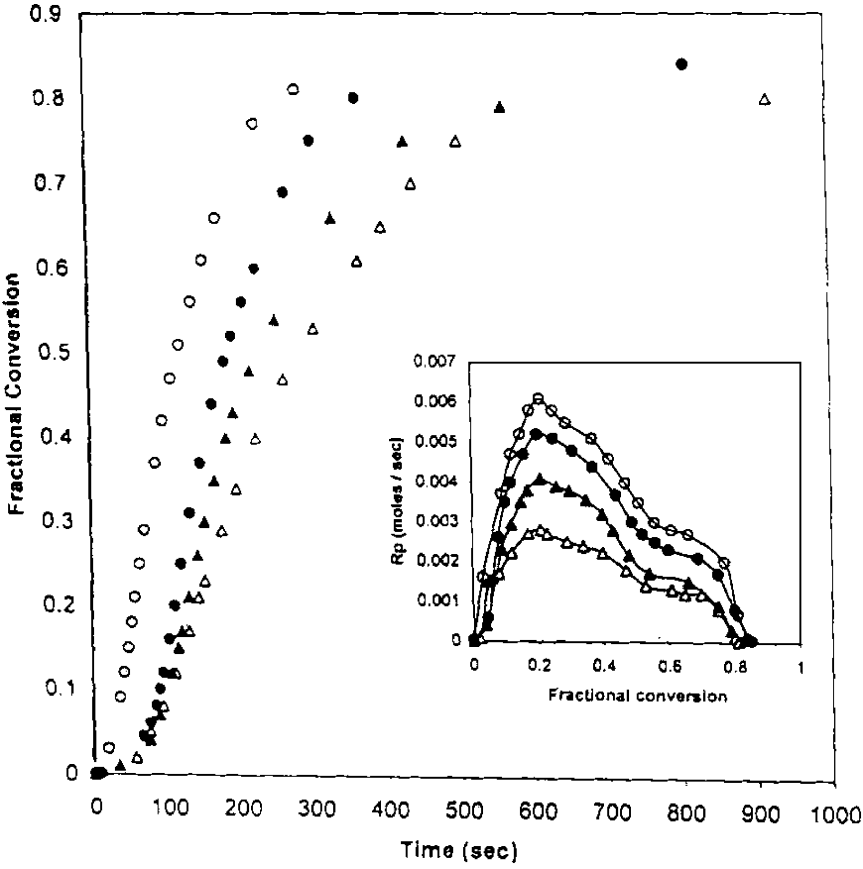

FIGURE 2 Effect of KPS concentration on % conversion and rate of polymerization at M/S = 0.66, temperature 70°C and EA (0.5)–MMA (0.5). (△) 0.18 Mm, (▲) 0.36 mM, (●) 0.55 mM, (○) 0.73 mM.

polymerization. The effect is reported to be significant at pH below 3 for KPS [12]. The observed pH at the interface of the micelles (which are the initiating sites) may be different than the measured pH due to enhanced or reduced concentration of hydrogen ion at the charged interface. When the reaction was performed under buffered conditions in the presence of 3 mM $NaHCO_3$ at a controlled pH of 8.4, the final conversion increased to 96% and particle size decreased to 80 nm from 130 nm observed for an unbuffered system. Similar observation has also been reported by Morgan et al. [13] where it was demonstrated that conversion can reach nearly 100% by controlling the pH for the

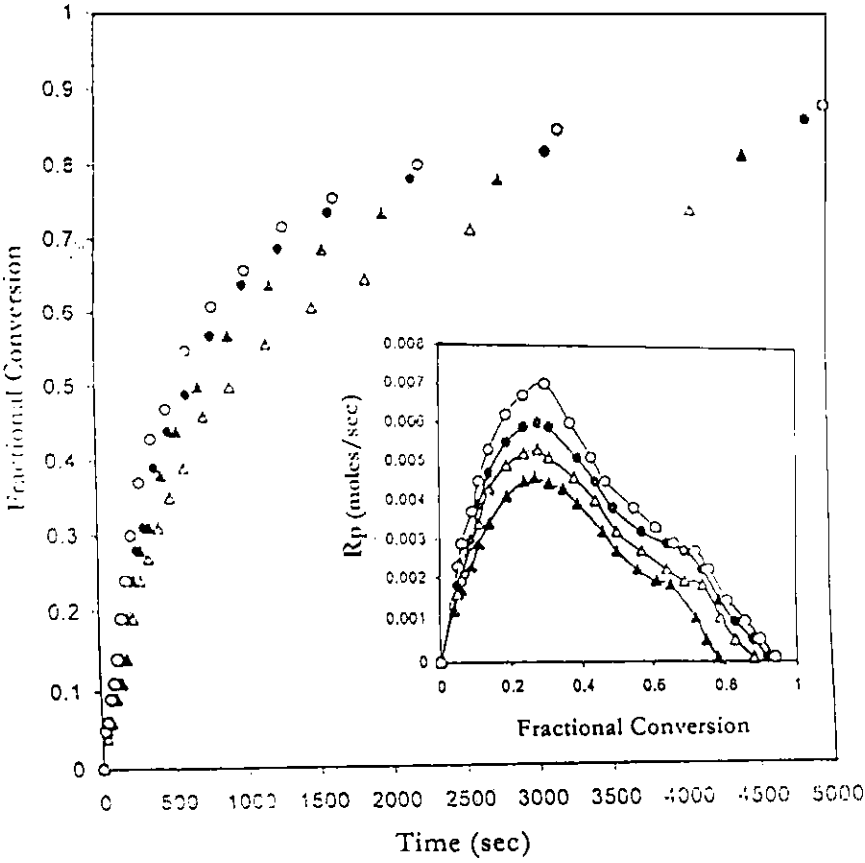

FIGURE 3 Effect of AIBN concentration on % conversion and rate of polymerization at M/S = 0.66, temp 70°C and EA (0.5)–MMA (0.5). (△) 0.18 mM, (▲) 0.36 mM, (●) 0.55 mM, (○) 0.73 Mm.

microemulsion polymerization of hexylmethacrylate initiated with KPS. However, the AIBN-initiated system resulted in lower particle size (compared to KPS initiated system) at the same M/S ratio, temperature, and molar concentration of intiator (Figure 4a and b). This is surprising because the decomposition rate constant k_d of AIBN at 70°C is 1.27×10^{-4} [14], which is lower than KPS [5.01×10^{-2}] [14] at the same temperature. Hence, a lesser number of polymer particles having larger particle size are expected for AIBN initiation. A lower particle size for AIBN indicates greater number of effective radicals initiating polymerization and hence a higher rate of polymerization and Np/ml as compared to the KPS initiated system (Table 1).

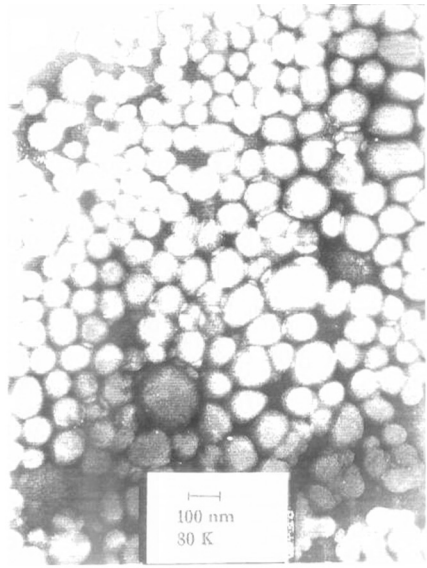

(a)

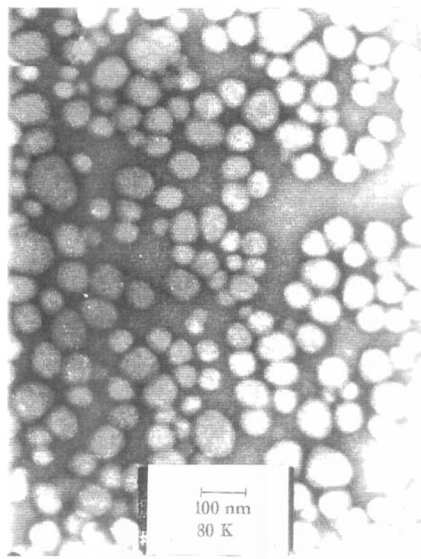

(b)

FIGURE 4 (a) TEM at 85% conversion of a sample synthesized through microemulsion polymerization of EA (0.5)–MMA (0.5) using 0.73 mM KPS at 25°C at 80 K magnification. (b) TEM at 95% conversion of a sample synthesized through microemulsion polymerization of EA (0.5)–MMA (0.5) using 0.73 mM AIBN at 80 K magnification.

TABLE 1 Kinetic and Colloidal Parameters for Microemulsion Copolymerization of EA MMA at 70°C using 0.73 mM KPS and AIBN

Fractional conversion	Rate, moles/s	Dn in nm	Np/cm^3	$\bar{n}$	PI
M:S = 0.66 [KPS]					
0.11	0.0046	56	9.8×10^{13}		0.07
0.37	0.0051	31	1.94×10^{15}	4.19	0.064
0.50	0.0034	36	1.84×10^{15}	4.81	0.060
0.67	0.0026	47	1.01×10^{15}	5.73	0.069
0.75	0.002	57	6.18×10^{14}		0.077
0.84	0.00003	124	1.1×10^{14}		0.18
M/S = 0.66 [AIBN]					
0.42	0.006	27	3.2×10^{15}	1.0	0.09
0.50	0.0045	33	2.13×10^{15}	1.4	0.10
0.85	0.0014	48	1.2×10^{15}		0.10
0.90	0.00007	55	8.45×10^{14}		0.04

$\bar{n}$ is average number of radical per particle; PI is the polydispersity index.

Radical generation from AIBN is generally explained on the basis of a single radical produced either from the very small portion of the initiator dissolved in aqueous phase or radical desorption from the microdroplets or monomer swollen micelles unless they recombine within the droplet. It seems that a smaller size of the microdroplet (leading to an increased surface area) favors single radical formation by radical desorption. However, more work is necessary to arrive at a definite conclusion, whereas the observed decrease in Np for KPS initiated microemulsion can be (Table 1) due to particle agglomeration, as seen in TEM (Figure 4b). This also leads to an observed broad particle size distribution (PSD) at 85% conversion (Figure 5c). Figures 5 and 6 show the variation in PSD with conversion for microemulsion systems initiated with both KPS and AIBN. A monomodal distribution for lower conversion samples irrespective of initiator type, indicates a predominantly single nucleation mechanism that is widely accepted to be the microemulsified droplets. This, however, does not rule out the possibility of a homogeneous nucleation, particularly for polar monomers. In fact, Kim and Napper [15] have shown that a more sensitive technique like fluorescence can distinguish between the competitive nucleation mechanisms, whereas the contribution of homogeneous nucleation in an emulsion system can be traced using the conventional techniques.

Emulsion copolymerization of EA–MMA (1:1 mole ratio) represented by point B and C of the phase diagram was carried out at M/S ratios 10 and 50. Figures 7 and 8 show the conversion versus time

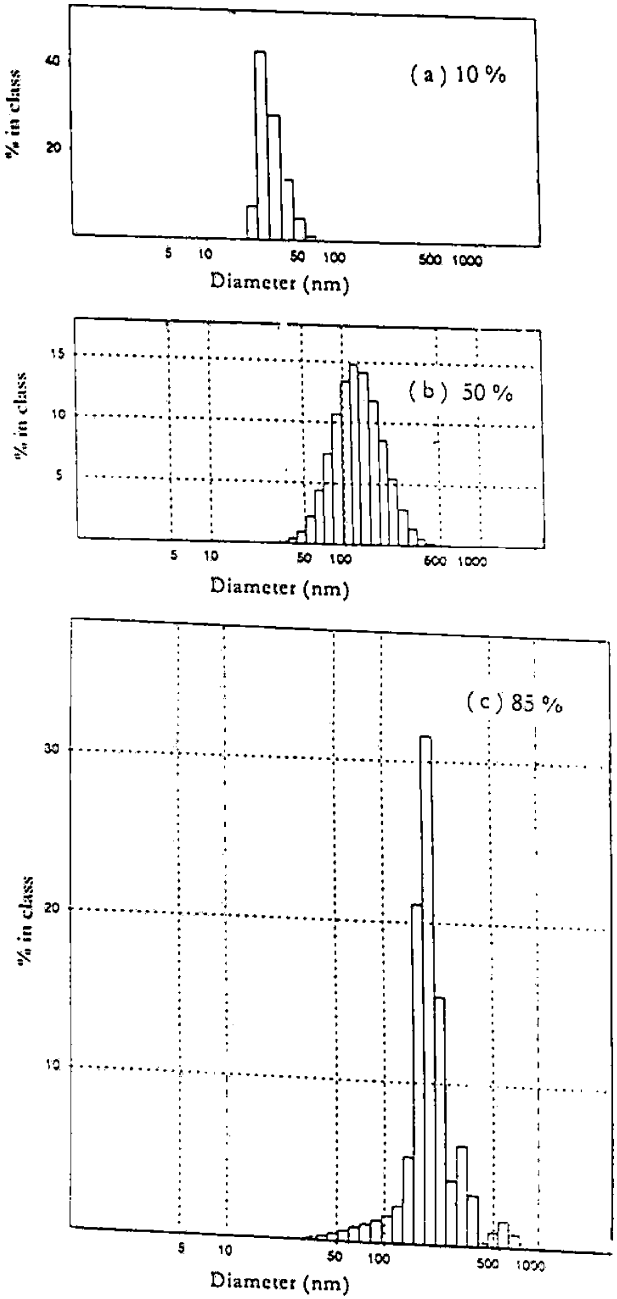

FIGURE 5 Particle size distribution for KPS initiated system at three different stages of microemulsion polymerization. EA (0.5)–MMA (0.5), 0.73 mM KPS, 25°C, M/S = 0.66.

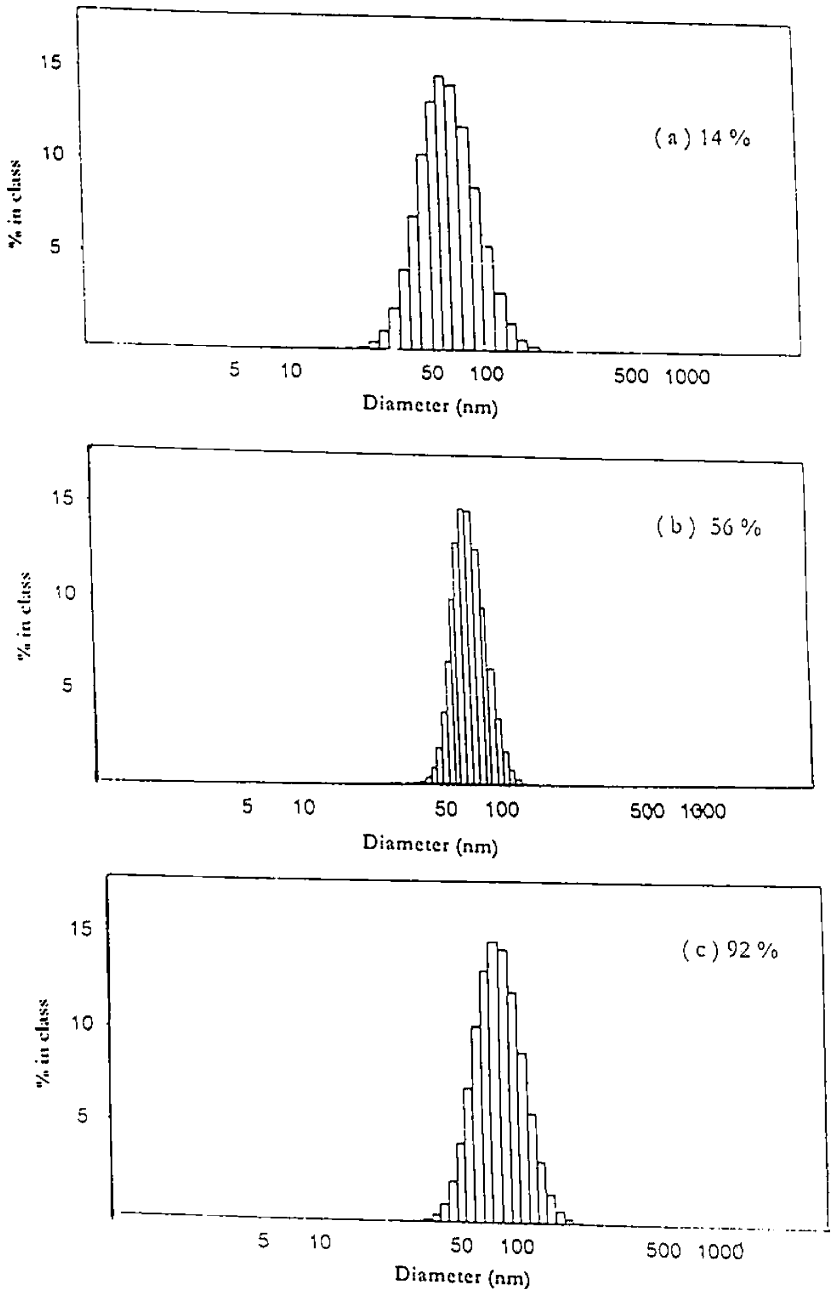

FIGURE 6 Particle size distribution for AIBN initiated system at three different stages of microemulsion. EA (0.5)–MMA (0.5), 0.73 mM AIBN, 25°C, M/S = 0.66.

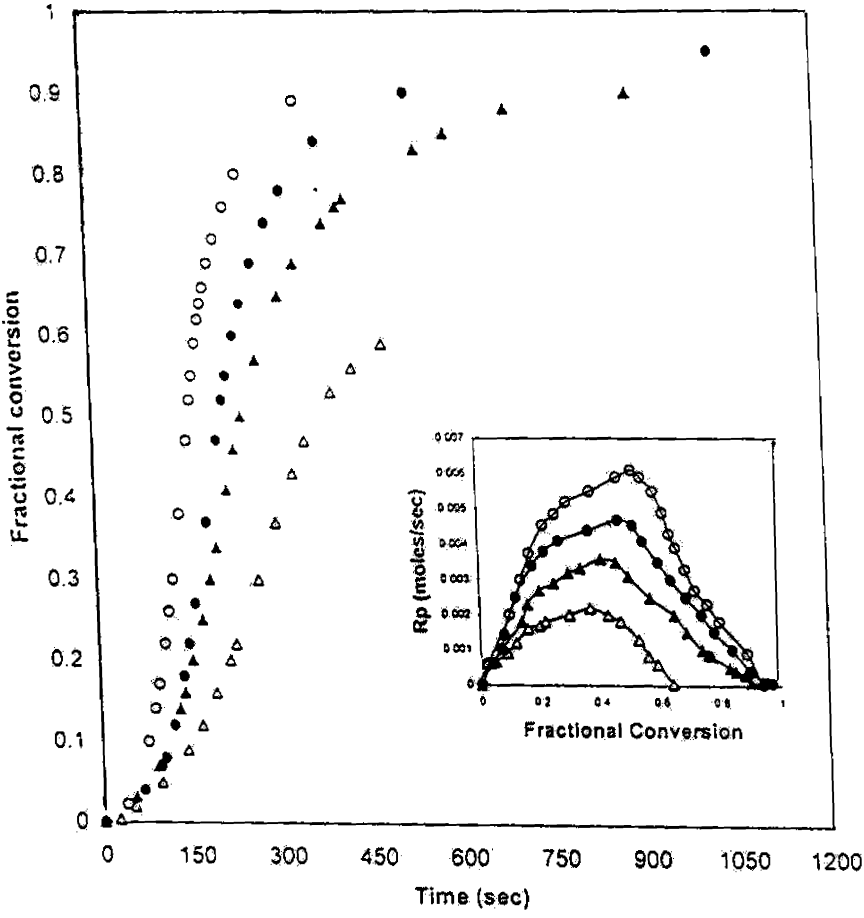

FIGURE 7 Effect of KPS concentration on % conversion and rate of polymerization at M/S = 10, at T = 70°C and EA (0.5)–MMA (0.5). (△) 0.18 mM, (▲) 0.36 mM, (●) 0.55 mM, (○) 0.73 mM.

and Rp versus conversion plots for M/S = 10 and 50, respectively. These emulsions turned into stable, translucent nanosized latexes, when 0.73 mM KPS was used at 70°C. Such a transition was not observed with AIBN at the same M/S ratio, AIBN concentration, and temperature. Instead, the system showed phase separation at around 70% conversion. This can be attributed to the lower decomposition rate constant (k_d) of AIBN at 70°C compared to KPS at the same temperature, and the availability of lower concentration of AIBN dissolved in water in the initiation of emulsion polymerization. This

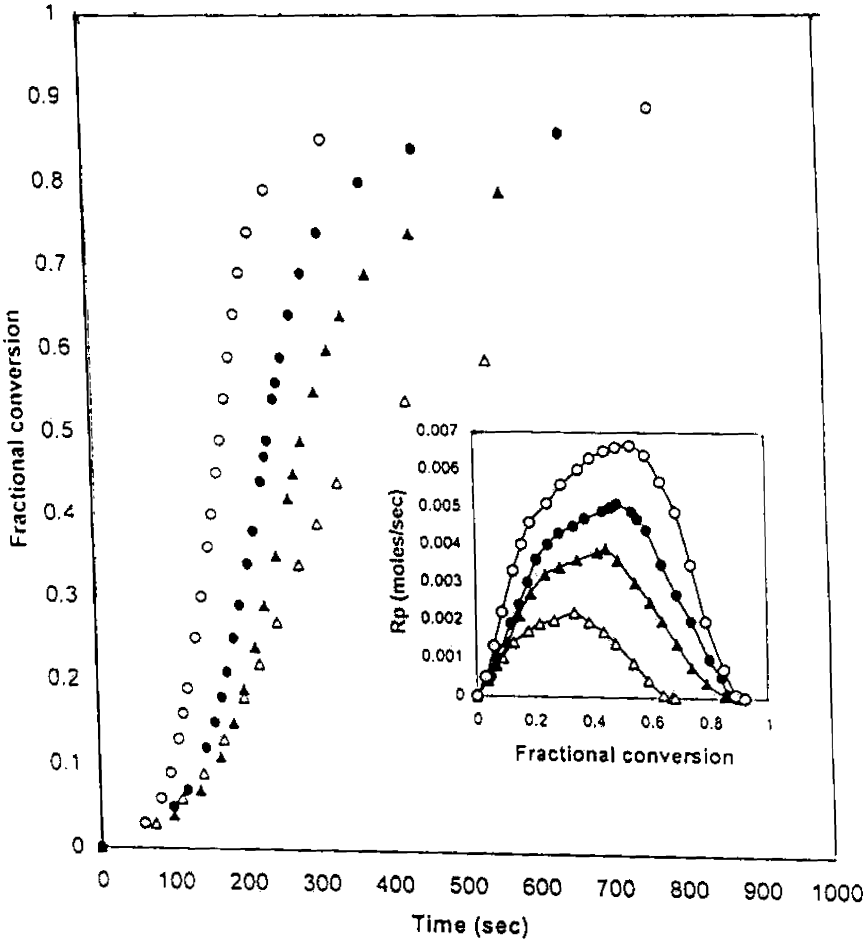

FIGURE 8 Effect of KPS concentration on % conversion and rate of polymerization at M/S = 50, at T = 70°C and EA (0.5)–MMA (0.5). (△) 0.18 Mm, (▲) 0.36 mM, (●) 0.55 mM, (○) 0.73 mM.

leads to a lesser number of active radicals initiating polymerization resulting in the generation of a lesser number of polymerization sites. Diffusion of monomer from monomer droplets and uninitiated micelles results in the particle growth. The rate of coagulation is also expected to be higher compared to KPS initiated system due to the absence of surface charge at the polymer chain end. The combination of these facts renders the available surfactant insufficient, resulting in a phase separation.

Initiation of an emulsion polymerization system with the water-soluble initiator KPS generates oligomeric radicals formed in aqueous phase that can enter the monomer swollen micelles only after the attainment of a critical chain length or hydrophobicity at which it becomes surface active [16]. This can increase their residence time at the micelle–water interface and hence the probability of radical entry. For the present system, the critical chain length for entry was calculated from hydrophobic free energy consideration using Maxwell's model [17]:

$$z = 1 - 23 \text{ kJ mol}^{-1}/\text{RT ln } C_w^{sat}$$

where, z is the average degree of polymerization for entry and C_w^{sat} is the saturated aqueous phase concentration of the monomer in mol dm^{-3}. The saturated water solubility reported for EA and MMA is 1.8% and 1.5%, respectively [18]. The average value of C_w^{sat} was used for calculation, because 0.5 mole fraction of each monomer was taken for kinetic studies. The value of z was observed to be 6. Further addition of monomer units in the aqueous phase results in the increase in hydrophobic free energy of the surfactant making it hydrophobic enough not to form a micelle but to precipitate out to generate new particle the in the aqueous phase leading to homogeneous nucleation. It has been reported [16] that the critical degree of polymerization for homogeneous nucleation, j_{crit}, can be calculated from the consideration of hydrophobic free energy of the surfactant having the same Kraft temperature as the temperature of the emulsion polymerization under study. This leads to

$$i_{crit} = 1 - 55 \text{ kJ mol}^{-1}/\text{RT ln } C_w^{sat}$$

The value of j_{crit} for the present system was observed to be 12 at 70°C. The fact that polymer particles are generated by both micellar and homogeneous nucleation is evident from the following studies.

The Rp versus Conversion plots (Figures 7 and 8) show a prolonged nucleation period and the absence of a constant rate period. Because the conversion of micelles into polymer particles takes place at lower conversion, the further slower increase in the rate of polymerization can be attributed to particle nucleation in aqueous phase (homogeneous nucleation). TEM (Figure 9a) for a 50% conversion sample (soon after the system turned translucent) shows a large number of smaller particles, most likely to be generated by homogeneous nucleation for $M/S = 50$ system. The slower increase in rate due to particles, generated through homogeneous nucleation has been attributed to reduced swelling of the particles by monomer due to their

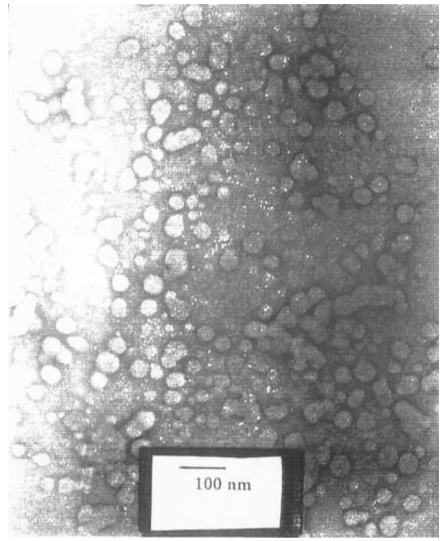

(a)

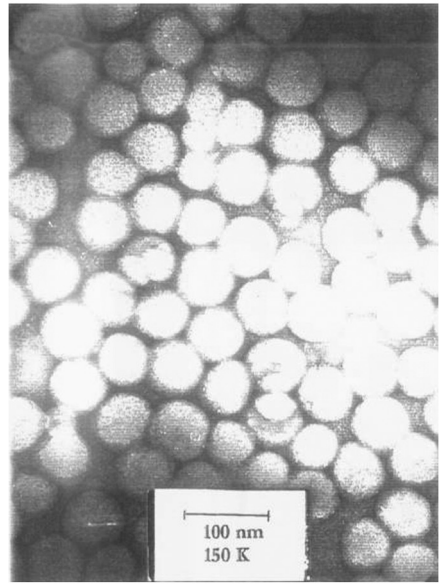

(b)

FIGURE 9 (a) TEM of a sample synthesized through emulsion polymerization of EA (0.5)–MMA (0.5) using 0.73 mM KPS at M/S = 50 and 80 K magnification at 50% conversion. (b) TEM of sample synthesized through emulsion polymerization of EA (0.5)–MMA (0.5) initiated with 0.73 mM KPS at M/S = 50 and 150 K magnification at 97% conversion.

hydrophilic character and rapid exit of free radicals due to their small size. Simultaneous diffusion of monomer into the particles, generated via micellar and homogeneous nucleation, results in the disappearance of monomer as a separate phase by the time the rate maxima are achieved. Due to higher rate of particle nucleation, particle growth kinetics becomes less important in these emulsion systems involving both partially water soluble monomers. Two-stage kinetics in emulsion polymerization has been reported even in the case of styrene and SDS as a surfactant by Varela de la Rosa et al. [19] where the conversion was monitored by a microcalorimeter. Gan et al. [20] also have reported two stage kinetics in the emulsion polymerization of styrene and MMA. To the best of the present authors' knowledge, no reports have tried to explain such an observation.

The particle size distribution at 4%, 27%, and 57% conversion for M/S = 50 clearly shows a bimodal nature (Figure 10a–c) indicating particle generation through two nucleation mechanisms. Table 2 shows the final number of particles (Np/ml) for the system with M/S ratios 10 and 50. The number of particles were observed to increase initially and thereafter remained nearly constant. The particles generated by homogeneous nucleation are relatively unstable in a colloidal state, which is reported to arise as a consequence of their small size and the extreme curvature of the electrical double layer [21]. Therefore, the particles are prone to coagulative events, resulting in a slight decrease in the Np/cm^3 (Table 2), and a slight increase in particle size and increase in monodispersity as seen in TEM (Figure 9b) and particle size distribution (Figure 10d).

Therefore, the role of KPS and AIBN varies in the emulsion and microemulsion systems, depending on their preferential distribution in aqueous or organic phase as well as on the relative importance of droplet and homogeneous nucleation for the overall particle nucleation of both systems. Kinetic details indicated that homogeneous nucleation has a greater contribution to latex particle formation in emulsion system compared to microemulsion. The earlier point is substantiated more quantitatively by ^{1}H NMR and DSC measurements.

Copolymer Composition through ^{1}H NMR

Even the small difference in solubility of EA (1.8%) and MMA (1.5%) has shown a considerable influence on the copolymer composition, as seen from NMR studies and thermal properties. The copolymer composition data for emulsion polymerization obtained by ^{1}H NMR at various feed compositions and below 10% conversion are given in Table 3. The copolymers synthesized through emulsion polymerization

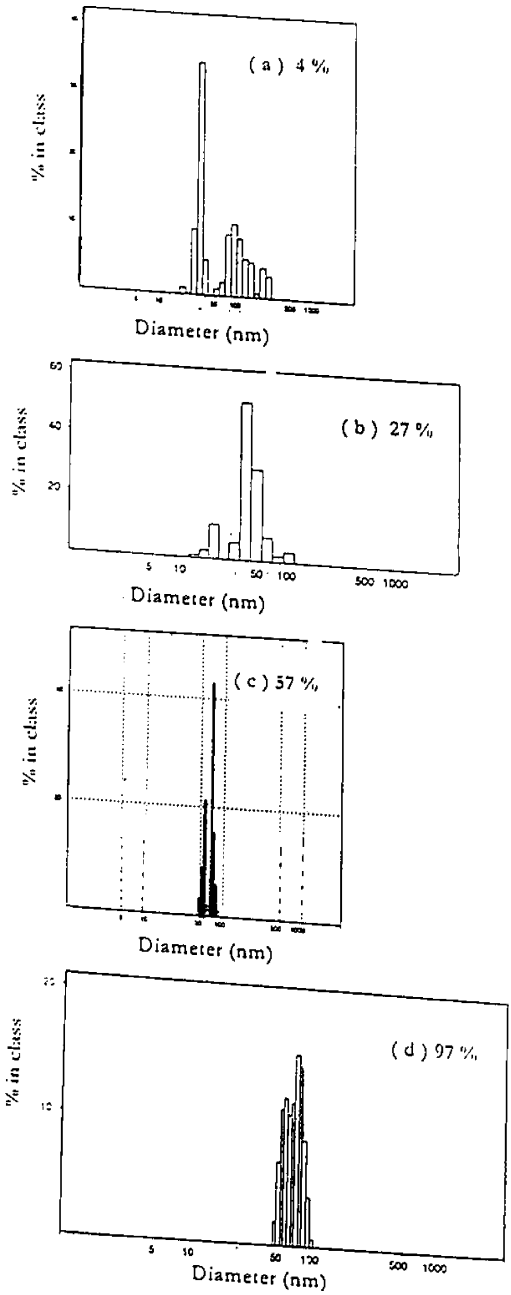

FIGURE 10 Particle size distribution of EA (0.5)–MMA (0.5) copolymer synthesized through emulsion polymerization at M/S = 50 at various conversion initiated with 0.73 mM KPS. (a) 4%, (b) 27%, (c) 57%, (d) 97%.

TABLE 2 Kinetic and Colloidal Parameters for Emulsion Copolymerization of EA MMA at 70°C using 0.73 mM KPS

Fractional conversion	Rate moles/s	Dn in nm	Np/cm^3	$\bar{n}$	PI
M:S = 10					
0.18	0.0038	28	1.35×10^{15}	4.66	0.13
0.41	0.0056	33	1.88×10^{15}	4.13	0.11
0.76	0.0025	36	2.7×10^{15}	1.38	0.10
0.89	0.0009	38	2.7×10^{15}	—	0.11
0.95	0.0001	37	3.06×10^{15}	—	0.11
M:S = 50					
0.05	0.0011	30	7.58×10^{14}	—	0.39
0.17	0.0041	35	1.62×10^{15}	2.79	0.08
0.56	0.0065	46	2.3×10^{15}	3.73	0.08
0.70	0.0049	50	2.3×10^{15}	2.81	0.05
0.86	0.0007	54	2.3×10^{15}	—	0.08
0.92	0.0001	57	2.03×10^{15}	—	0.11
0.97	0.00002	59	1.99×10^{15}	—	0.10

$\bar{n}$ is average number of radical per particle; PI is the polydispersity index.

contained a greater fraction of the more water-soluble monomer EA in comparison to the copolymer synthesized by bulk polymerization of EA-MMA for identical feed concentration and below 10% conversion. This indicates that the composition drift in emulsion polymerization, arises due to the initiation of polymerization in both aqueous phase and micelles. In addition, the contribution of homogeneous nucleation to the overall particle nucleation increases with decrease in the surfactant concentration. Therefore, copolymer composition studied

TABLE 3 Comparison of Copolymer Composition Below 10% Conversion for Emulsion and Bulk Copolymerization of EA–MMA

Feed concentration		Emulsion, M/S = 50		Emulsion, M/S = 10		Bulk[25]	
f_{EA}	f_{MMA}	F_{EA}	F_{MMA}	F_{EA}	F_{MMA}	F_{EA}	F_{MMA}
0.90	0.10	0.81	0.19	0.76	0.24	0.72	0.27
0.75	0.25	0.58	0.42	0.54	0.46	0.51	0.49
0.66	0.33	0.48	0.52	0.43	0.57	0.42	0.57
0.50	0.50	0.35	0.65	0.32	0.68	0.30	0.70
0.25	0.75	0.19	0.81	0.14	0.86	0.13	0.86
0.10	0.90	0.10	0.90	0.06	0.94	0.05	0.94

f_{EA}, f_{MMA}: Feed concentrations of ethylacrylate and methylmethacrylate.
F_{EA}, F_{MMA}: Ethylacrylate and methylmethacrylate fraction in copolymer.

TABLE 4 Comparison of Copolymer Composition Below 10% Conversion for Microemulsion and Bulk Copolymerization of EA–MMA

Feed concentration		Microemulsion, M/S = 0.66		Bulk[41]	
f_{EA}	f_{MMA}	F_{EA}	F_{MMA}	F_{EA}	F_{MMA}
0.9	0.1	0.73	0.27	0.72	0.28
0.75	0.25	0.52	0.48	0.51	0.49
0.66	0.33	0.39	0.61	0.42	0.58
0.50	0.50	0.30	0.70	0.30	0.70
0.25	0.75	0.13	0.87	0.13	0.87
0.1	0.90	0.05	0.95	0.05	0.95

f_{EA}, f_{MMA}: Feed concentrations of ethylacrylate and methylmethacrylate.
F_{EA}, f_{MMA}: Ethylacrylate and methylmethacrylate fraction in copolymer.

at M/S = 10 for conversion below 10% and at various compositions shows lesser drift in copolymer composition from bulk copolymerization as compared to M/S = 50 (Table 3). Upon increasing the surfactant concentration further for microemulsion polymerization at M/S = 0.66, a negligleble drift in copolymer composition was observed when the results were compared to bulk polymerization at similar feed concentrations and below 10% conversion (Table 4). A drift in copolymer composition of a microemulsion system could not be traced as the effect has been subdued by little difference in the relative solubility of the comonomers and lesser degree of homogeneous nucleation compared to an emulsion system. A representative ^{1}H NMR for EA–MMA copolymer is given in (Figure 11).

Thermal Properties by DSC

The copolymers synthesized through emulsion polymerization show two Tgs (Figure 12 and Table 5). The appearance of two Tgs can be attributed to the formation of a diblock copolymer due to large difference in their monomer reactivities [$r_{MMA} = 1.44$, $r_{EA} = 0.25$] [22]. However, such a possibility can be denied when the polymer characterization is done below 10% conversion and the copolymer synthesized in microemulsion showed a single Tg (Figure 12). Hence, the appearance of two Tgs indicates the formation of copolymer chains with two different compositions arising from micellar and homogeneous nucleation. The polymer generated via micellar polymerization is expected to have a greater fraction of the less water-soluble monomer, MMA, and corresponds to the higher Tg, whereas homogeneous

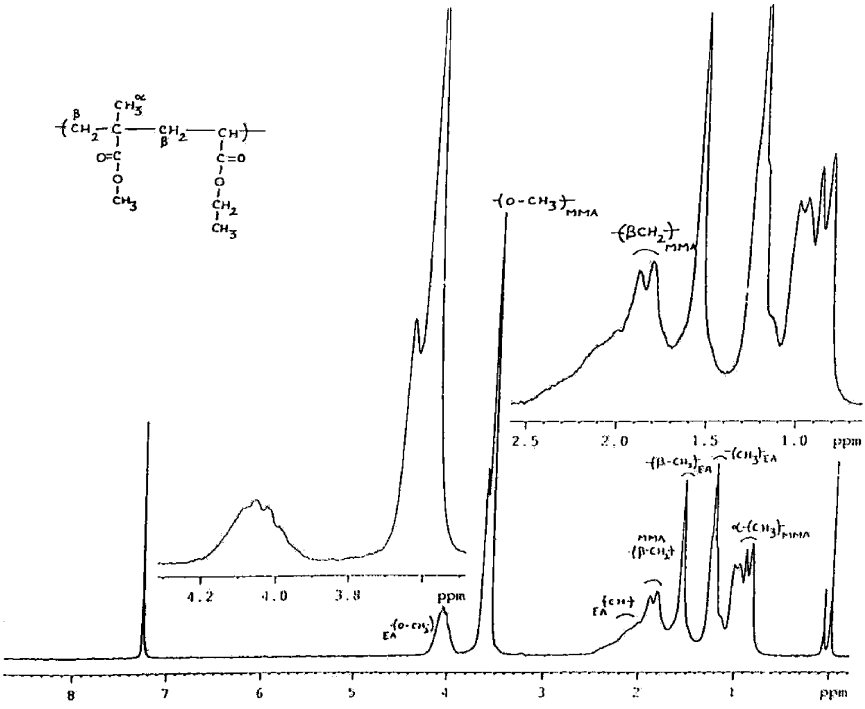

FIGURE 11 ^{1}H NMR spectrum of EA–MMA copolymers synthesized through emulsion polymerization. MMA in feed 0.5 and in copolymer 0.651.

nucleation generates polymer chains with higher fraction of the more water soluble monomer, EA, resulting in the lower Tg. The difference in the observed Tgs is significant due to the large difference in the Tgs of the homopolymers, Whereas copolymers synthesized through microemulsion polymerization show a single Tg, indicating a predominance of a single copolymerization locus (Figure 12).

Probable Termination Events

The number of radicals per particle ($\bar{n}$) for the system under study was calculated using the following equation, and the results are given in Tables 1 and 2.

$$\overline{n} = \frac{Rp(c) \times Np \times (kp_{EA} \times r_{MMA} + kp_{MMA} \times r_{EA} \times L) \times (1 + L)}{[M]eq \times kp_{MMA} \times kp_{EA} \times N_o \times (r_{MMA} + 2L + r_{EA} \times L^2)}$$

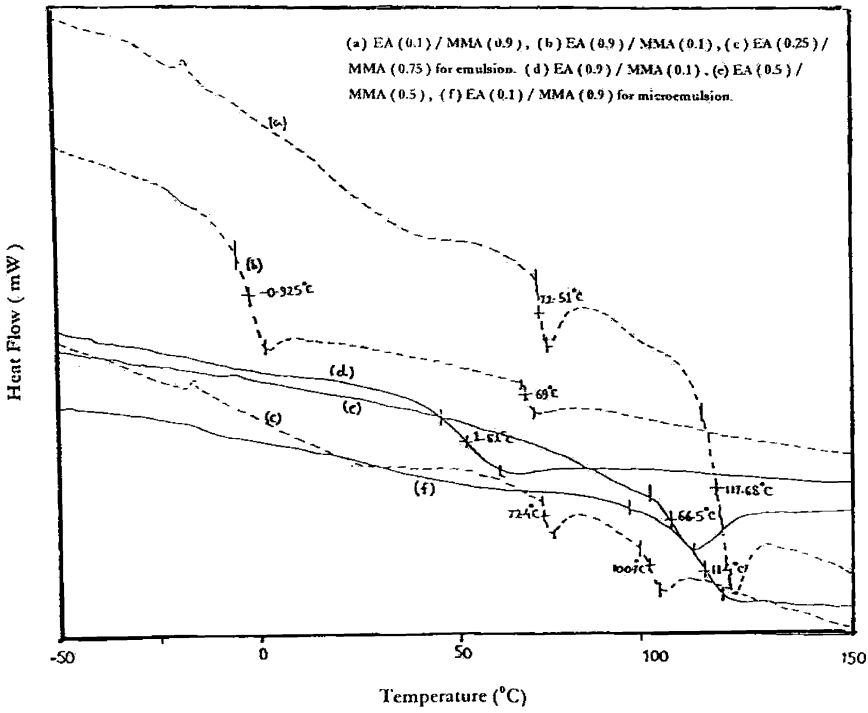

FIGURE 12 DSC thermograms of EA–MMA copolymer synthesized through emulsion and microemulsion polymerization at three different composition. (- - - - - -) Emulsion, (————) Microemulsion. (a) EA (0.1)/MMA (0.9), (b) EA (0.9)/MMA (0.1), (c) EA (0.25)/MMA (0.75), (d) EA (0.9)/MMA (0.1), (e) EA (0.5)/MMA (0.5), (f) EA (0.1)/MMA (0.9).

where Rp(c) is the copolymerization rate, [M]eq is the equilibrium monomer concentration, taken as 6.0 mol/dm^3 as reported by Capek and Tuan [9] from the swelling studies of the final MMA–EA

TABLE 5 Glass Transition Temperature for Copolymers Below 10% Conversion Through Emulsion Polymerization of EA–MMA

Feed composition		At M/S = 10		At M/S = 50	
EA	MMA	Tg_1°C	Tg_2°C	Tg_1°C	Tg_2°C
0.25	0.75	72	100	68	102
0.50	0.50	69	91	62	86
0.75	0.25	28	66	23	71
0.90	0.10	0.30	50	–1.0	68

copolymer latexes. The reported propagation rate constant [kp] values of 1,500 and 686 $dm^3\,mol^{-1}sec^{-1}$, for EA and MMA have been used for the calculation of $\bar{n}$. The monomer ratio [EA]/[MMA], is represented as L. Reactivities of EA and MMA used for the calculation in emulsion medium are reported to be 0.25 and 1.44, respectively by us [22] N_p/cm^3 is the number of particles calculated from Equation 1 using dynamic light scattering data. N_o is the Avogadro number.

Table 1 shows a relatively high value of $\bar{n}$ in the microemulsion polymerization initiated with KPS. Gardon [23] reported as high as five radicals per particle in the emulsion polymerization of MMA. Figure 13 and Table 6 give the molecular weight distribution and molecular weights for the emulsion and microemulsion systems.

The polymer synthesized through microemulsion polymerization has a larger fraction of low molecular weight polymer chains, which is in contrast to what is generally reported in case of microemulsion polymerization where the molecular weight can reach as high as 10^6–10^7. The number of polymer chains per particle [N_p] calculated from the weight of the polymer in each milliliter of microemulsion was also found to be 1279. Similar results were reported by Pilcher and Ford [24] for the microemulsion polymerization of MMA

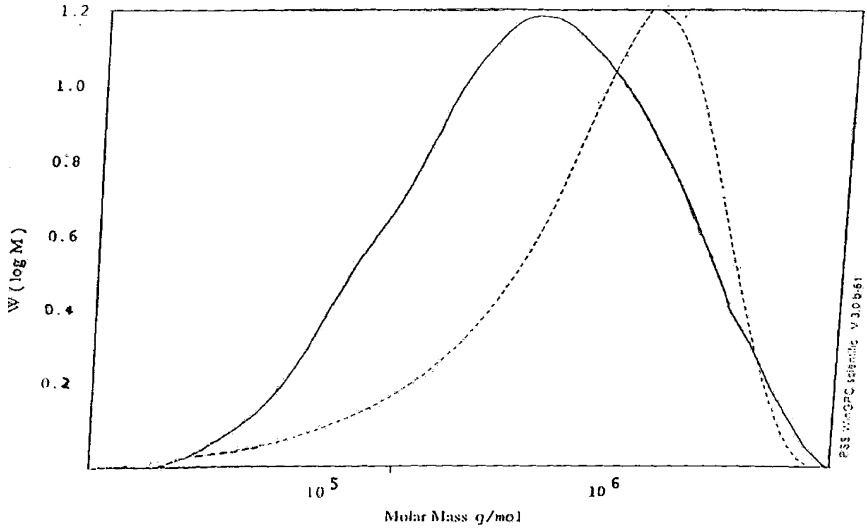

FIGURE 13 Molecular Weight distribution of copolymers synthesized through microemulsion emulsion polymerization at M/S = 10 and 50, EA (0.5)–MMA (0.5), KPS = 0.73 mM for emulsion (. . . . . .) and at M/S = 0.66, EA (0.5)–MMA (0.5), KPS = 0.73 mM for microemulsion. (- - - - - - - - - -).

TABLE 6 Molecular Weights for Emulsion- and Microemulsion-Based Copolymers

	Microemulsion		Emulsion	
Molecular weight	M/S = 0.66 [KPS]	M/S = 0.66 [AIBN]	M/S = 10 [KPS]	M/S = 50 [KPS]
Mn	9.1×10^4	5.6×10^5	5.19×10^5	1.34×10^6
Mw	2.4×10^5	1.0×10^6	1.63×10^5	5.09×10^5
Mw/Mn	2.6	1.9	3.17	2.64

($N_p = 1034$). The higher value of N_p can arise due to the combined effect of coagulation leading to increase in particle size and radical accumulation (also suggested by a higher value of $\bar{n}$, Table 1) at higher conversion. Radical accumulation is due to the inability of the radicals to terminate (which is diffusion controlled) due to the combined effect of closeness of Tg and reaction temperature, larger particle size, and increased microviscosity due to solubility of polymer in the monomer. The earlier condition might lead to unimolecular termination through chain transfer to the monomer and surfactant as the operative termination mechanism for microemulsion polymerization initiated with KPS. The AIBN-initiated microemulsion system gives value of N_p equal to 540, which is due to the smaller particle size (Table 1) and higher molecular weight (Table 6) compared to the KPS-initiated system. In comparison to microemulsion, emulsion systems with M/S ratio 10 and 50, show much lower value of N_p and lower fraction of low molecular weight fractions. The N_p values were observed to be 35 and 135, respectively. The lower particle size and higher number of particles can make radical exit more facile. Subsequent bimolecular termination and chain transfer to the desorbed radical can take place either in aqueous phase or by reentry into the growing radical.

CONCLUSION

Relative contribution of homogeneous nucleation to the process of particle formation, especially for polar monomers, becomes significant at lower surfactant concentration. This has been realized on studying the copolymerization of polar monomers employing the same molar concentration of the water-soluble initiator KPS and the oil-soluble initiator AIBN. Simultaneous particle formation through homogeneous and heterogeneous nucleation for emulsion system initiated with water-soluble initiator KPS initially produced a greater number

of polymer particles stabilized by the available surfactant. Apart from the kinetic results, this has been substantiated by ^{1}H NMR and DSC. The copolymers isolated at the nucleation stage showed a higher rate of particle nucleation for KPS-initiated emulsion system. This allows a lower particle size to be achieved at higher monomer concentration, whereas the same concentration of AIBN resulted in a phase separation and much higher concentration was required to generate a stable latex system.

On the contrary, the KPS initiated microemulsion system showed a significant particle growth due to a lower number of effective radical initiating species, compared to the AIBN-initiated system. Gel effect was observed at higher conversions for both KPS- and AIBN-initiated microemulsions.

Thus, the role of initiator partitioning in the different phases of polymerization, in conjuction with the number of stable polymer particles produced, and its subsequent stabilization by the surfactant, plays an important role in determining the final latex properties such as solid content and stability.

REFERENCES

[1] Jaikrishnan, A. and Shah, D. O., *J. Polym. Sci. Polym. Lett.* **22**, 31 (1984).
[2] Gou, J. S., Sudol, E. D., Vanderhoff, J. W., and El-Aasser, M. S., *J. Polym. Sci. Part A: Polym. Chem.* **30**, 703 (1992).
[3] Gou, J. S., Sudol, E. D., Vanderhoff, J. W., and El-Aasser, M. S., *J. Polym. Sci. Part A: Polym. Chem.* **30**, 691 (1992).
[4] Priest, W. J., *J. Phy. Chem.* **56,** 1077 (1952).
[5] Bleger, F., Murthy, A. K., Pla, F., and Kaler, E. W., *Macromolecules* **27**, 2559 (1994).
[6] Harkins, W. D., *J. Am. Chem. Soc.* **69**, 1428 (1947).
[7] Gan, L. M., Chew, C. H., Lee, K. C., and Ng, S. C., *Polymer* **34**, 3064 (1993).
[8] Rodriguez–Guadarrama, L. A., Mendizabal, E., Puig, J. E., and Kaler, E. W., *J. Appl. Polym. Sci.* **48**, 775 (1993).
[9] Capek, I. and Tuan, L. Q., *Macromolecules* **187**, 2063 (1986).
[10] Bhawal, S., Dhoble, D., and Devi, S., *J. Appl. Polym. Sci.* **90**, 2593 (2003).
[11] Behrman, E. J. and Edwards, J. O., *Rev. Inorg. Chem.* **2**, 179 (1980).
[12] Kolthoff, I. M., Bovey, F. A., Medalia, A. I., and Meehan, E. J. (1955). *Emulsion Polymerisation*, Interscience Publisher, New York.
[13] Morgan, J. D., Lusvardi, K. M., and Kaler, E. W., *Macromolecules* **30**, 1897 (1997).
[14] Brandrup, J. and Immergut, E. H. (eds.), (1989). *Polymer Handbook*, 3rd ed., Wiley, New York.
[15] Kim, D. R. and Napper, D. H., *Macromol. Rapid Commun.* **17**, 845 (1996).
[16] Gilbert, R. G. (1995). *Emulsion Polymerisation: A Mechanistic Approach*, Academic Press, New York, pp. 309.
[17] Maxwell, I. A., Morrison, B. R., Napper, D. H., and Gilbert, R. G., *Macromolecules* **24**, 1629 (1991).
[18] Lovell, P. A. and El-Aasser, M. S. (1997). *Emulsion Polymerisation and Emulsion Polymers*, John Wiley, New York, pp. 211.

[19] Varela de la Rosa, L., Sudol, E. D., El-Aasser, M. S., and Klein, A., *J. Polym. Sci. Part A, Polym. Chem.* **34**, 461 (1996).
[20] Gan, L. M., Chew, C. H., Ng, S. C., and Loh, S. E., *Langmuir* **9**, 2799 (1993).
[21] Feeney, P. J., Napper, D. H., and Gilbert, R. G., *Macromolecules* **17**, 2520 (1984).
[22] Bhawal, S. and Devi, S., *J. Appl. Polym. Sci.* **86**, 2802 (2002).
[23] Gardon, J. L., *J. Polym. Sci.* A-1, **6**, 628 (1968).
[24] Pilcher, S. C. and Ford, W. T., *Macromolecules* **31**, 3454 (1998).
[25] Gressie, N., Torrance, B. J. D., and Fortune, J. D., *Polymer* **6**, 665 (1965).